

SURFACE PLASMONS

https://doi.org/10.1070/QEL16454

Multimode theory of plasmon excitation at a metal–photonic crystal interface

T.I. Kuznetsova, N.A. Raspopov

Abstract. **Surface plasmon excitation at a photonic crystal–metal interface is studied taking into account multiple scattering of an initial light wave on a periodical crystal structure. The analysis is focused on calculating characteristics of the eigenwaves in a one-dimensional crystal, which comprise a set of harmonics with the wavevectors separated from each other by the value of the crystal lattice wavevector. Reflection from the crystal–metal interface binds the amplitudes of propagating and evanescent modes. Calculations show that for the dielectric characteristics of a synthetic opal and a substrate made of a real metal with a ruby laser radiation used as the initial wave, the fulfilment of plasmon resonance conditions leads to a local increase in the surface plasmon amplitude by a factor of 6.4–9 as compared to the average amplitude of the initial wave. As a rule, the effect can only be obtained for a single surface wave, all other waves being substantially weaker than the main plasmon. There is a specific case where the resonance condition holds for two modes simultaneously. In this case, two oppositely directed fluxes of equal intensity are generated at the interface. The resonance condition breaks at a small deviation of the incident angle of the initial wave θ from the normal direction ($|\theta| \geqslant 10^{-4}$ rad). In the latter case, the picture is asymmetric: at angles $|\theta| \geqslant 5\times10^{-3}$ rad, only one plasmon remains intensive. The local density of electromagnetic energy at the photonic crystal–metal interface may exceed the corresponding value of the initial wave by a factor of 40–80.**

Keywords: *photonic crystal, evanescent modes, surface plasmon intensity.*

1. Introduction

There is a series of works reporting the principal possibility of exciting surface plasmons in various optical schemes [1–16]. In contrast to classical schemes [17] (which employ a total internal reflection prism or corrugated metal surface), other variants were also considered. Plasmon generation on a hole in a metal screen, on a system of screen holes, on walls of a cylindrical or planar waveguide and on an output flange of a waveguide was discussed. In the last decade, attention has been paid to plasmon excitation on photonic crystal faces. Variation of crystal reflection and transmission coefficients observed experimentally near a metallic plate or film was considered as a manifestation of plasmon influence [18–24]. The process of plasmon excitation was not discussed in these works.

We have established [25, 26] that transformation of the initial wave to the plasmon requires a thorough study of the structure of optical modes in the crystal. In [25, 26], we started a theoretical study of waves in such systems and estimated the efficiency of transforming initial waves incident onto the crystal input surface to plasmons at output surface. A one-dimensional photonic crystal was considered; as seed waves we have chosen the waves propagating either in parallel or at a small angle to the crystal layers (Fig. 1b). The modulation factor of the dielectric function was taken close to that of widely used globular crystals – synthetic opals, that is, noticeably less than unity. These parameters are estimated in [26]. In these conditions, the initial plane wave acquires, as a rule, a weak component due to scattering on medium irregularities and has an increased value of the wavevector. There is also a second eigenwave, in which the component with a large value of the wavevector prevails and a small component has the transverse structure of the initial wave. The first eigenwave (mode) is the propagating one, whereas the second eigenwave is evanescent.

Analysis of the boundary conditions for the waves at the crystal–metal interface, which takes into account both the eigensolutions, yields amplitudes of the wave reflected from the boundary and of the surface wave propagating along the interface. Calculations show that under optimal conditions the amplitude of the surface wave at the interface may exceed that of the initial propagating wave by a factor of 5–6. This occurs [25, 26] at the values of the dielectric functions of the two media and at the angle of initial wave incidence close to the plasmon resonance conditions [17]. Restrictions to these characteristics are strict: for example, deviation from the optimal angle of initial wave incidence by 5×10^{-3} rad reduces the amplitude of the plasmon wave by an order of magnitude. Hence, resonances in the system are very narrow. Calculation results strongly depend on variations of problem parameters and the question arises as to the dependence of this effect on the number of interacting waves considered. Kuznetova and Raspopov [25, 26] used a well known two-wave approach [27, 28] as a basis. It is not clear whether the estimates obtained in the two-wave approximation can answer the question on a reachable coefficient of transformation of the initial propagating wave to the surface plasmon.

In the present work, we present a multiwave theory of radiation passage through a photonic crystal with plasmon origin when the radiation reflects from a crystal–metal interface. Calculations based on the theory suggested will confirm a high efficiency of the scheme with a photonic crystal for generating surface plasmons.

T.I. Kuznetsova, N.A. Raspopov P.N. Lebedev Physical Institute, Russian Academy of Sciences, Leninsky prosp. 53, 119991 Moscow, Russia; e-mail: tkuzn@sci.lebedev.ru, rna@sci.lebedev.ru

Received 19 June 2017; revision received 25 August 2017
Kvantovaya Elektronika **47** (12) 1171–1177 (2017)
Translated by N.A. Raspopov

2. Problem statement. Optical modes in a crystal

Consider a photonic crystal unbounded in the directions of the coordinate axes x and y. The crystal has an interface with a metal substrate along the plane $z = 0$. The dependence of the crystal dielectric function has the form $\varepsilon(x) = \varepsilon_0 + \tilde{\varepsilon}[\exp(iGx) + \exp(-iGx)]$, that is, the period of the crystal lattice is $L = 2\pi/G$. Medium properties are independent of the coordinates y and z. A light wave falls onto the crystal. Note that in theoretical studies of one-dimensional photonic crystals it is customary to consider waves propagating in the direction normal to crystal layers, that is, along the gradient ε (Fig. 1a). However, there are works concerning two-dimensional problems. For example, nonlinear interaction of radiation with a photonic crystal was studied in [29] under inclined wave incidence to the crystal. The problem required two-dimensional consideration. The present work requires solving a two-dimensional problem as well. Here we consider the case where the incident wave passes at a small angle with respect to the crystal layers (Fig. 1b) or even along the layers, that is, normally to the gradient ε. In addition, only two-wave interaction is conventionally considered in the literature [27, 28] including our works [25, 26]. In the present work, we include into consideration five partial waves with the wavevector x-components $\{k_x - 2G, k_x - G, k_x, k_x + G, k_x + 2G\}$ and the sought-for components k_z and magnetic field amplitudes $\{H_{-2}, H_{-1}, H_0, H_1, H_2\}$.

Issuing from known wave equation for TM-waves in an inhomogeneous medium [30] we obtain the equation for the y-component of the magnetic field H

$$\Delta H + \frac{\omega^2}{c^2}\{\varepsilon_0 + \tilde{\varepsilon}[\exp(iGx) + \exp(-iGx)]\}H - \frac{1}{\varepsilon}\frac{\partial\varepsilon}{\partial x}\frac{\partial H}{\partial x} = 0. \quad (1)$$

Taking into account a small value of the modulation depth relative to the average value of the dielectric function $\tilde{\varepsilon}/\varepsilon_0 \equiv \xi$ we obtain from (1) the equations for the amplitudes of five partial waves:

$$\begin{aligned}
&\left[\varepsilon_0\frac{\omega^2}{c^2} - (k_x - 2G)^2 - k_z^2\right]H_{-2} + \xi\left[\varepsilon_0\frac{\omega^2}{c^2} - G(k_x - G)\right]H_{-1} = 0,\\
&\xi\left[\varepsilon_0\frac{\omega^2}{c^2} + G(k_x - 2G)\right]H_{-2} + \left[\varepsilon_0\frac{\omega^2}{c^2} - (k_x - G)^2 - k_z^2\right]H_{-1} + \xi\left(\varepsilon_0\frac{\omega^2}{c^2} - Gk_x\right)H_0 = 0,\\
&\xi\left[\varepsilon_0\frac{\omega^2}{c^2} + G(k_x - G)\right]H_{-1} + \left(\varepsilon_0\frac{\omega^2}{c^2} - k_x^2 - k_z^2\right)H_0 + \xi\left[\varepsilon_0\frac{\omega^2}{c^2} - G(k_x + G)\right]H_1 = 0, \quad (2)\\
&\xi\left(\varepsilon_0\frac{\omega^2}{c^2} + Gk_x\right)H_0 + \left[\varepsilon_0\frac{\omega^2}{c^2} - (k_x + G)^2 - k_z^2\right]H_1 + \xi\left[\varepsilon_0\frac{\omega^2}{c^2} - G(k_x + 2G)\right]H_2 = 0,\\
&\xi\left[\varepsilon_0\frac{\omega^2}{c^2} + G(k_x + G)\right]H_1 + \left[\varepsilon_0\frac{\omega^2}{c^2} - (k_x + 2G)^2 - k_z^2\right]H_2 = 0.
\end{aligned}$$

The wavenumber component k_z that is the same for all the components with different k_x is to be found. To simplify formulae, we divide system of equations (2) by ω^2/c^2 and transfer to dimensionless wavevector components $g = Gc/\omega$, $v = k_x c/\omega$, $u = k_z c/\omega$. The coordinates x and z are accordingly renormalised. Now the matrix for system of equations (2) takes the form for the magnetic field components $\{H_{-2}, H_{-1}, H_0, H_1, H_2\}$ (3).

Now we will find eigenvalues $U_j = u_j^2$ and eigenvectors of matrix (3). According to the rank of the matrix we have five eigenvectors $\{f_1, f_2, f_3, f_4, f_5\}$. The functions f_j are linear combinations of simple waves: $f_j = \sum \mu_{jn} h_n$, where h_n refer to the partial waves mentioned above. We may write functions h_n using positive indices:

$$\{h_1, h_2, h_3, h_4, h_5\} = \{\exp[i(v - 2g)x], \exp[i(v - g)x], \exp(ivx), \exp[i(v + g)x], \exp[i(v + 2g)x]\}.$$

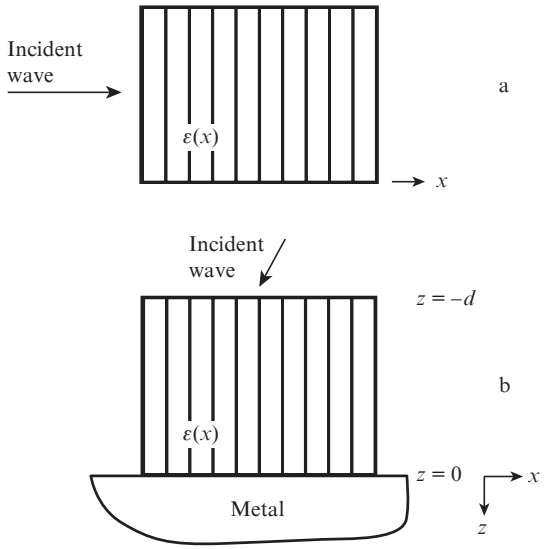

Figure 1. Propagation direction of a light wave falling onto a photonic crystal. (a) Standard scheme and (b) scheme of the present work.

$$\begin{pmatrix}
\varepsilon_0 - (v - 2g)^2 - u^2 & \xi[\varepsilon_0 - g(v - g)] & 0 & 0 & 0\\
\xi[\varepsilon_0 + g(v - 2g)] & \varepsilon_0 - (v - g)^2 - u^2 & \xi(\varepsilon_0 - gv) & 0 & 0\\
0 & \xi[\varepsilon_0 + g(v - g)] & \varepsilon_0 - v^2 - u^2 & \xi[\varepsilon_0 - g(v + g)] & 0\\
0 & 0 & \xi(\varepsilon_0 + gu) & \varepsilon_0 - (v + g)^2 - u^2 & \xi[\varepsilon_0 - g(v + 2g)]\\
0 & 0 & 0 & \xi[\varepsilon_0 + g(v + g)] & \varepsilon_0 - (v + 2g)^2 - u^2
\end{pmatrix}. \quad (3)$$

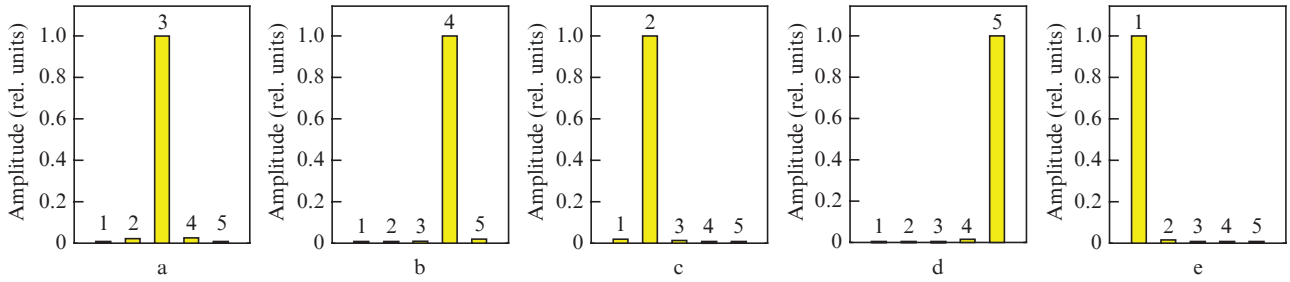

Figure 2. Normalised amplitudes of partial waves comprised in various modes of the photonic crystal. The angle between the direction of initial wave propagation and normal to the crystal surface is $\theta = \arcsin(-0.25)$; parameters of the medium are given in the text. Numbers of partial waves $\{1, 2, 3, 4, 5\}$ refer to the wavenumbers $\{k_x - 2G, k_x - G, k_x, k_x + G, k_x + 2G\}$. Pictures corresponding to various modes are ordered according to reducing eigennumbers U_j: (a) $U_1 = 1.787$, (b) $U_2 = -0.1666$, (c) $U_3 = -1.836$, (d) $U_4 = -7.692$ and (e) $U_5 = -11.031$.

The new functions f_j are modes of an inhomogeneous medium in the crystal under consideration. We take medium characteristics typical for a synthetic opal in the visible spectral range: $\varepsilon_0 = 1.851$, $\xi = 0.035$. Let the absolute values of the lattice dimensionless wavevector g be within the limits 0.5–1.5 and those of the dimensionless x-component of the initial wavevector be in the interval $-0.7 \leqslant v \leqslant 0.7$. In this case, all the off-diagonal elements in the matrix are substantially less than diagonal ones. Hence, in each of the functions f_j, one simple wave prevails, whereas factors at other waves are substantially smaller. Specific features of the modes obtained for the medium with mentioned dielectric function characteristics will be considered in Section 4 (Fig. 2). Note that the weak waves comprised in the modes cannot be neglected; only making allowance for these waves can explain the transformation of the initial wave to evanescent waves.

3. Boundary conditions. Basic system of equations

By using the eigenfunctions discussed in Section 2, we describe a semirestricted domain ($z \leqslant 0$). The magnetic field inside the crystal is presented in the form

$$H(x,z) = \sum_{j=1}^{5} F_j f_j(x) \exp(w_j z) + H_{\text{refl}}(x,z), \tag{4}$$

where $w_j = \sqrt{-U_j}$;

$$f_j(x) = \sum_{n=1}^{5} \mu_{jn} h_n(x); \tag{5}$$

F_j are constants; and H_{refl} is a sum of reflected modes; while calculating the square root for $U_j > 0$, the product of the positive number to the imaginary unit is taken, and for $U_j < 0$ the positive number is chosen. Thus, propagating waves pass from $-\infty$ in the positive direction of the z axis, and evanescent waves attenuate in the negative direction of the z axis. Propagating waves can generate reflected waves with inverted dependence on z at the interface. For evanescent waves, there are no waves inverted in z. In the calculations, only such parameter sets are considered, which give one solution for matrix (3) in the form of a propagating mode, whereas the other solutions refer to evanescent modes. We will use the subscript m to denote the single propagating wave and the amplitude of the corresponding reflected wave will be written as F_{refl} so that expression (4) for the field inside crystal will take the form

$$H(x,z)\big|_{z\leqslant 0} = \sum_{j=1}^{5} [F_j \exp(w_j z) + \delta_{jm} F_{\text{refl}} \exp(-w_j z)] f_j(x). \tag{6}$$

From (6) and (5) follows

$$H(x,z)\big|_{z\leqslant 0} = \sum_{j=1}^{5} [F_j \exp(w_j z) + \delta_{jm} F_{\text{refl}} \exp(-w_j z)] \times \sum_{n=1}^{5} \mu_{jn} h_n(x). \tag{7}$$

Now consider the domain $z > 0$. In this case, the medium is homogeneous (metal) and the field H in it can be presented as a single sum

$$H(x,z)\big|_{z\geqslant 0} = \sum_{n=1}^{5} \sigma_n h_n(x) \exp(-\gamma_n z), \tag{8}$$

where σ_n are the wave amplitudes, and

$$\gamma_n = \sqrt{(v + ng - 3g)^2 - \varepsilon_{\text{met}}} \tag{9}$$

are attenuation constants in metal.

In contrast to (4), the choice of square root sign in (9) is obvious. By making (7) and (8) equal at $z = 0$, we obtain the expression for the y-component of the magnetic field

$$\sum_{j=1}^{5} (F_j + \delta_{jm} F_{\text{refl}}) \sum_{n=1}^{5} \mu_{jn} h_n(x) = \sum_{n=1}^{5} \sigma_n h_n(x). \tag{10}$$

From (10) follows that factors at each of the functions $h_n(x)$ should be equal. Finally, we obtain the first boundary condition – the continuity condition for $H(x,z)$ in the form of five equations:

$$\sum_{j=1}^{5} (F_j + \delta_{jm} F_{\text{refl}}) \mu_{jn} = \sigma_n, \quad 1 \leqslant n < 5. \tag{11}$$

Let us pass to the second boundary condition. We find expressions for the values, to which the tangential electric field components are proportional in two domains, namely, for the parameters $\varepsilon^{-1} \partial H/\partial z$ at $z = 0$. In the domain $z < 0$ we use the expansion of ε, and the product takes the form

$$\frac{1}{\varepsilon} \frac{\partial}{\partial z} H(x,z)\big|_{z\leqslant 0} \approx \frac{1}{\varepsilon_0} \left\{ 1 - \frac{\tilde{\varepsilon}[\exp(igx) + \exp(-igx)]}{\varepsilon_0} \right\} \frac{\partial}{\partial z} H\big|_{z\leqslant 0}. \tag{12}$$

In view of (7) and (12) we have

$$\frac{1}{\varepsilon}\frac{\partial}{\partial z}H\Big|_{z=-0} = \frac{1}{\varepsilon_0}\sum_{j=1}^{5} w_j (F_j - \delta_{jm}F_{\text{refl}}) \times \sum_{n=1}^{5}\Big(\mu_{jn} - \frac{\tilde{\varepsilon}}{\varepsilon_0}\mu_{jn+1} - \frac{\tilde{\varepsilon}}{\varepsilon_0}\mu_{jn-1}\Big)h_n(x). \quad (13)$$

This formula comprises factors μ_{jn}, some of which refer to harmonics neglected in our calculations. In further calculations, the factors corresponding to such harmonics are assumed zero $\mu_{j0} = \mu_{j6} = 0$. Other coefficients μ_{jn} are calculated by the method from Section 2.

In the domain $z > 0$ such problems are absent and from (8) we obtain

$$\frac{1}{\varepsilon}\frac{\partial}{\partial z}H\Big|_{z=+0} = -\frac{1}{\varepsilon_{\text{met}}}\sum_{n=1}^{5}\gamma_n\sigma_n h_n(x). \quad (14)$$

By making (13) and (14) equal we find

$$-\frac{1}{\varepsilon_{\text{met}}}\sum_{n=1}^{5}\gamma_n\sigma_n h_n(x) = \frac{1}{\varepsilon_0}\sum_{j=1}^{5} w_j (F_j - \delta_{jm}F_{\text{refl}}) \times \sum_{n=1}^{5}\Big(\mu_{jn} - \frac{\tilde{\varepsilon}}{\varepsilon_0}\mu_{jn+1} - \frac{\tilde{\varepsilon}}{\varepsilon_0}\mu_{jn-1}\Big)h_n(x). \quad (15)$$

From (15) follows that the factors at each of the waves $h_n(x)$ $(1 \leqslant n \leqslant 5)$ in both sides of the equality should coincide. Thus, the second boundary condition takes the final form

$$-\frac{1}{\varepsilon_{\text{met}}}\gamma_n\sigma_n = \frac{1}{\varepsilon_0}\sum_{j=1}^{5} w_j (F_j - \delta_{jm}F_{\text{refl}}) \times \Big(\mu_{jn} - \frac{\tilde{\varepsilon}}{\varepsilon_0}\mu_{jn+1} - \frac{\tilde{\varepsilon}}{\varepsilon_0}\mu_{jn-1}\Big). \quad (16)$$

By combining both boundary conditions (11) and (16) and excluding unknown amplitudes σ_n we obtain the system of equations

$$\sum_{j=1}^{5} w_j (F_j - \delta_{jm}F_{\text{refl}})\Big(\mu_{jn} - \frac{\tilde{\varepsilon}}{\varepsilon_0}\mu_{jn+1} - \frac{\tilde{\varepsilon}}{\varepsilon_0}\mu_{jn-1}\Big) + \frac{\varepsilon_0}{\varepsilon_{\text{met}}}\gamma_n\sum_{j=1}^{5}(F_j + \delta_{jm}F_{\text{refl}})\mu_{jn} = 0. \quad (17)$$

System (17) obtained is a basis for numerical simulations.

4. Calculation results

Numerical simulations were performed for a number of particular examples according to the algorithm described above. We take the average value of the crystal dielectric function $\varepsilon_0 = 1.851$ and its relative modulation depth $\xi = 0.035$. The exciting wave is the radiation of a ruby laser at the wavelength $\lambda = 694$ nm, the period of the crystal lattice is $L = 0.6\lambda$, and the absolute value of the lattice wavevector is $G = 1.6698\,\omega/c$. The crystal is placed on a silver substrate; the dielectric function of silver at the wavelength of the incident wave is $\varepsilon_{\text{met}} = -22.6367 + 0.4013\text{i}$ [31]. For the angle of incidence of the initial wave we take $\theta = \arcsin(-0.25)$, for the x-component of the scattered wave we have $v = -0.25$. Note that these parameter values obey the equality

$$v + g = \text{Re}\Big(\frac{\varepsilon_0\varepsilon_{\text{met}}}{\varepsilon_0 + \varepsilon_{\text{met}}}\Big) = 1.4198 \equiv \text{Re}\Big(K_{\text{spp}}\frac{c}{\omega}\Big), \quad (18)$$

where K_{spp} is the wavenumber of a resonance plasmon [17]. Equality (18) at the parameters chosen provides the maximal proximity to the condition for plasmon resonance, which was derived for surface waves at the interface between two uniform media [17]. In our works [25,26] employing two-wave approximation, this condition provided the maximal plasmon intensity. One can easily write the condition, similar to (18), by making substitutions $v \to -v$, $K_{\text{spp}} \to -K_{\text{spp}}$, and $g \to -g$. It will be the resonance condition for a positive angle θ, which, in contrast to (18), refers to a plasmon propagating in the negative x-direction rather than in the positive one. Thus, it is clear that symmetry of the problem is not violated and the results obtained for negative angles θ can be expanded to the case of positive θ values as well.

We assume that in a multiwave system, as previously, the maximal plasmon amplitude should be sought for near the angle value satisfying equality (18). After substituting the parameters chosen above to matrix (3), the determinant of the matrix yields a quintic polynomial with respect to the square z-component of the wave vector $u^2 \equiv U$. There are five roots or five values U_j that turn the determinant to zero:

$$\{U_1, U_2, U_3, U_4, U_5\} = \{1.787, -0.1666, -1.836, -7.692, -11.031\}.$$

In what follows, the solutions are ordered according to falling values U_j. The following values w_j correspond to U_j:

$$w_j = \{1.337\text{i}, 0.408, 1.355, 2.774, 3.211\}.$$

In this raw, the first wave is propagating along the z axis and the other waves are evanescent. For each value of U_j there corresponds a set of amplitudes of partial waves, which is an eigensolution or, in other words, mode structure in the inhomogeneous medium. Figure 2 shows the calculated normalised amplitudes of partial waves comprised in particular modes. Data shown in Fig. 2a refer to the only mode, which propagates in the direction of the z axis. All other modes have imaginary z-components of wavevectors inside the crystal and attenuate with a distance from the crystal–metal interface; Figs 2b–2e refer to such modes. The results presented show that each mode comprises a selected partial wave with the factor substantially greater than factors at other waves. Now the eifenfunctions for unlimited crystal are found and we can describe a semirestricted medium and conjugation of the fields at the interface, that is, solve system of equations (17). The attenuation factors of partial waves in a homogeneous metal medium are calculated by using expression (9), and then one can pass to solving the main system of equations (17). The amplitude of the incident wave is taken unity and five other amplitudes are found. As a result, we obtain the absolute values of four plasmons and a reflected mode: $\{F_1, F_2, F_3, F_4, F_5, F_{\text{refl}}\} = \{1.0, 6.373, 0.0291, 0.0426, 0.0005, 0.934\}$ (the unit amplitude of the initial wave is the first in the list). The absolute value of the amplitude of the most intensive plasmon 6.37 is close to the value 6.50 obtained in our earlier work [26]. The other evanescent waves are substantially weaker than the 'main' plasmon.

We should verify whether the plasmon amplitude obtained is the maximal one for the crystal characteristics chosen and

the plasmon resonance condition provides the optimal regime in the system. We have performed similar calculations by varying the angle of incidence for the initial wave at the constant period of medium modulation $L = 0.6\lambda$. The dielectric functions of the two media are similar to previous calculations. Calculation results for dependence of the absolute value of the main plasmon amplitude are shown in Fig. 3 versus the angle of incidence. The dependence obtained is sharp, and the maximum position coincides with the value of resonance angle calculated above within an accuracy of 10^{-4} rad. The plasmon propagating in the negative x-direction has the maximal amplitude of 6.7; the calculated amplitude of a weaker plasmon propagating in the positive x-direction is 0.043. The amplitude of the reflected propagating wave is 0.93. The FWHM of the maximum is 4×10^{-3} rad. Hence, similarly to [25, 26], the determining role of plasmon resonance is confirmed.

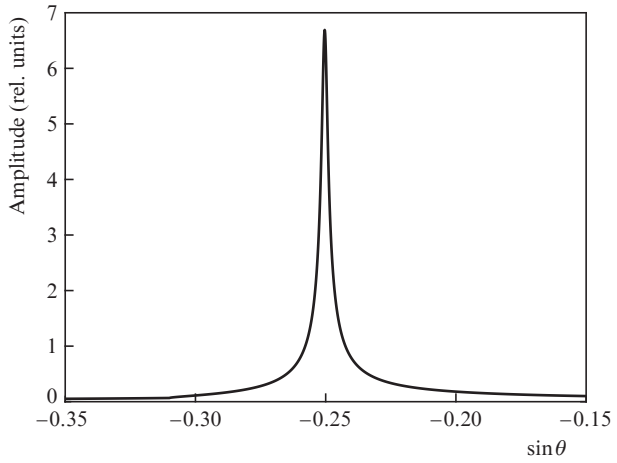

Figure 3. Absolute value of the amplitude of the main plasmon wave vs. sinus of the incident exciting wave angle $\sin\theta$ at $g = 1.6698$.

Now consider the case where the initial wave passes perpendicular to the surface $z = -d$. It means that the x-component of the initial wave is zero, $v = 0$. In contrast to the previous consideration, instead of (18), the following equality should hold

$$g = \mathrm{Re}\left(\frac{\varepsilon_0\varepsilon_{\mathrm{met}}}{\varepsilon_0 + \varepsilon_{\mathrm{met}}}\right) \equiv 1.4198. \qquad (19)$$

In matrix (3) by putting $v = 0$ for the modes of the modulated medium we obtain the matrix:

$$\begin{pmatrix} \varepsilon_0 - 4g^2 - u^2 & \xi(\varepsilon_0 + g^2) & 0 & 0 & 0 \\ \xi(\varepsilon_0 - 2g^2) & \varepsilon_0 - g^2 - u^2 & \xi\varepsilon_0 & 0 & 0 \\ 0 & \xi(\varepsilon_0 - g^2) & \varepsilon_0 - u^2 & \xi(\varepsilon_0 - g^2) & 0 \\ 0 & 0 & \xi\varepsilon_0 & \varepsilon_0 - g^2 - u^2 & \xi(\varepsilon_0 - 2g^2) \\ 0 & 0 & 0 & \xi(\varepsilon_0 + g^2) & \varepsilon_0 - 4g^2 - u^2 \end{pmatrix}. \qquad (20)$$

Properties of symmetry of this matrix due to the symmetry of directions $\pm x$ in the case of normal incidence allow one to transfer it to the quasi-diagonal form:

$$\begin{pmatrix} \varepsilon_0 - 4g^2 - u^2 & \xi(\varepsilon_0 + g^2) & 0 & 0 & 0 \\ \xi(\varepsilon_0 - 2g^2) & \varepsilon_0 - g^2 - u^2 & \sqrt{2}\,\xi\varepsilon_0 & 0 & 0 \\ 0 & \sqrt{2}\,\xi(\varepsilon_0 - g^2) & \varepsilon_0 - u^2 & 0 & 0 \\ 0 & 0 & 0 & \varepsilon_0 - g^2 - u^2 & \xi(\varepsilon_0 - 2g^2) \\ 0 & 0 & 0 & \xi(\varepsilon_0 + g^2) & \varepsilon_0 - 4g^2 - u^2 \end{pmatrix}. \qquad (21)$$

Omitting details, we present eigennumbers and mode structure expressed in terms of previous partial waves. For the eigennumbers we have the relation

$$U_j = \{1.8506, -0.1661, -0.1665, -6.2104, -6.2104\}.$$

These eigennumbers correspond to the following values w_j:

$$w_j = \{1.3604\mathrm{i}, 0.4076, 0.4080, 2.4921, 2.4921\}.$$

The mode structure for this case is shown in Fig. 4. One can see that each mode comprises partial waves with either similar amplitudes or amplitudes of equal absolute values and opposite signs. These modes are symmetric or antisymmetric solutions to equations (2) for fields in the modulated medium of the unlimited crystal. Note that the initial exciting wave is symmetric in x; hence, antisymmetric modes do not interact with it and are not pumped by it.

Now we can solve the main system of equations (17). In calculations, we take the amplitude of incident wave equal to unity and find amplitudes of the reflected wave and four pairwise symmetric running plasmons; each pair of symmetric plasmons forms a standing wave. Antisymmetric modes are not generated at normal incidence of the exciting wave. Calculation yields the following values: the absolute values of amplitudes for each of two oppositely directed main plasmons are 3.24, for two weak plasmons these are 0.021, and for the reflected wave it is 0.931 (the values are normalised to the

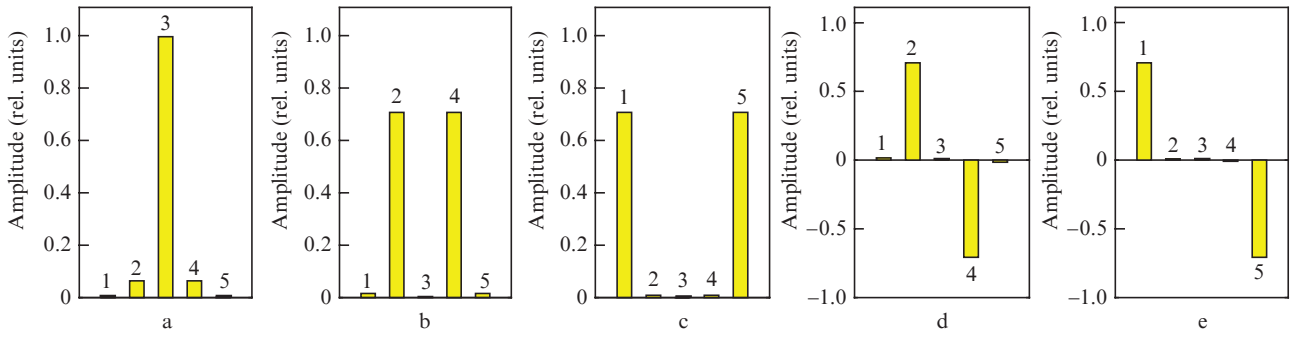

Figure 4. Normalised amplitudes of partial waves comprised in (a, b, c) symmetric and (d, e) antisymmetric modes of photonic crystal at normal incidence of the initial wave onto the crystal.

amplitude of the initial wave). The density of the electromagnetic energy flux normalised to that of the initial flux is 10 for each of the oppositely directed fluxes. The relative density of electromagnetic energy oscillates from zero in nodes to 40 in antinodes, the oscillation period coinciding with half the period of the crystal lattice.

Note that the pictures of excited fields in the case of normal incidence and incidence at the angle of $\theta = \arcsin(-0.25)$ strongly differ. In order to reveal how this transfer occurs in changing the angle of incidence we have performed detailed calculations over the whole intermediate range of angles. In the calculations, the lattice wavenumbers were taken such that resonance condition (18) holds for each incidence angle of the initial wave. Calculations show that in approaching the normal incidence up to the angle $\theta = \arcsin(-0.01)$, the amplitude of the main plasmon actually does not change, and other plasmons do not become noticeably stronger. In further reduction of angle θ, the picture substantially changes: the amplitude of the main plasmon strongly increases. In Fig. 5 one can see that it reaches 9.1 at the angle $\theta = -10^{-5}$ rad. Figure 5 also shows an increase in the amplitude of a weaker plasmon to the value of 4.7. Further approach of angle θ to zero and the corresponding reduction of the calculation steps result in irregular jumps of calculated values. This is explained by solution instability near $\theta = 0$ and requires another algorithm for calculating the mode structure. Practical employment of the specific behaviour of waves at very small angles seems rather interesting. However, the values of plasmon amplitudes obtained near zero incident angles should be averaged over the angular width of the exciting beam, which can hardly be made less than 5×10^{-5} rad because of the real crystal transverse dimensions. One can surely speak about plasmons with the amplitude of about 9.

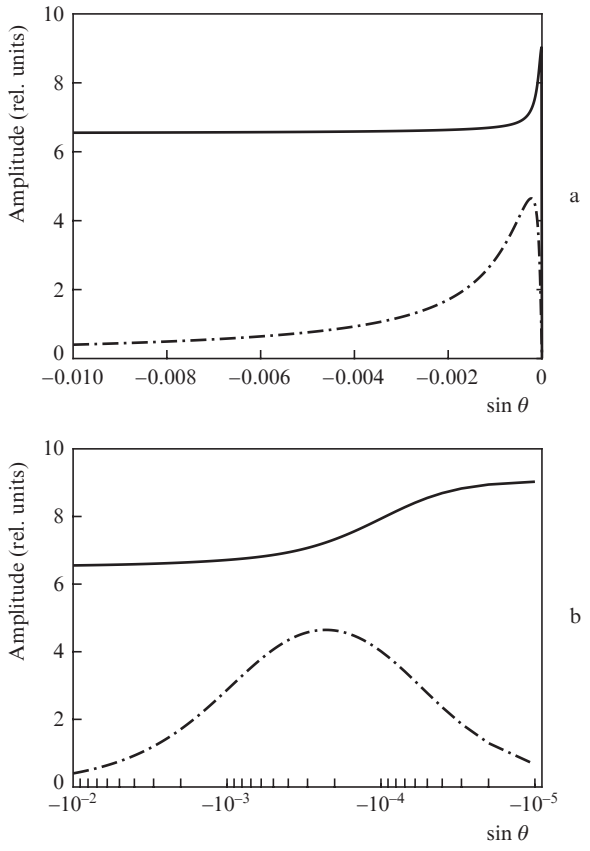

Figure 5. Absolute values of two main evanescent modes, which arise at the photonic crystal–metal interface ($z = 0$) when a propagating wave of unity intensity passes onto the interface vs. sinus of the angle of initial wave incidence $\sin\theta$ in (a) linear and (b) logarithmic scales of abscissa axis. Solid curves correspond to the mode with a prevailing wave having the wavenumber $k_x + G$, dash-and-dot curves refer to the case with a prevailing wave having the wavenumber $k_x - G$.

5. Conclusions

Efficiency of exciting surface plasmons in a synthetic opal in the visible spectral range is calculated. The method for studying optical modes in a crystal is developed, which takes into account multiple scattering of radiation on periodical inhomogeneities of the medium. Analysis allowed one to match multiple-component modes at the crystal–metal interface. The cases were found, where the multiple-wave approach is substantial. This occurs at such system parameters that the wavevectors of two waves participating in plasmon generation (including the initial and excited waves) have equal or close absolute values. In the problems considered, this occurs when the waves in the crystal undergo strong Bragg reflection. One of such variants is normal incidence of the initial wave onto a crystal (the wave propagation direction is parallel to crystal layers). In this case, a symmetric picture arises: two oppositely directed fluxes of energy of equal values. It is shown that at a small deviation of the exciting wave direction from normal incidence, the picture becomes asymmetrical. When the deviation from normal incidence is $|\theta| \geqslant 5\times10^{-3}$ rad, only one plasmon remains intensive. However, in the interval of angles $|\theta| \geqslant 10^{-4}-10^{-5}$ rad close to normal incidence, transformation of the propagating mode to the main surface plasmon is especially efficient. The field amplitude in the plasmon wave maximum may reach 6.4–9 relative to the initial wave amplitude. The local density of electromagnetic energy at the crystal–metal interface correspondingly increases by 40–80 times as compared to the initial wave.

Results of the present work show the possibility of employing the scheme presented for efficient generation of plasmons.

Acknowledgements. The authors are grateful to V.S. Lebedev for fruitful discussions.

The work was partially financially supported by the Russian Foundation for Basic Research (Grant No. 15-02-07777-a).

References

1. Ebbesen T.W., Lezec H.J., Chaemi H.F., Thio T., Wolff P.A. *Nature*, **391**, 667 (1998).
2. Laluet J.Y., Drezet A., Genet C., Ebbesen T.W. *New J. Phys.*, **10**, 105014 (2008).
3. Baudrion A.L., de Leon-Perez F., Mahbaub O., Hohenau A., Ditlbacher H., Garcia-Vidal F.J., Dintinger J., Ebbesen T.W., Martin-Moreno L., Krenn J.R. *Opt. Express*, **16**, 3420 (2008).
4. Kihm H.W., Lee K.G., Kim D.S., Ahn K.J. *Opt. Commun.*, **282**, 2442 (2009).
5. Dai W., Soukoulis C.M. *Phys. Rev. B*, **80**, 155407 (2009).
6. Nikitin A.Y., Rodrigo S.G., Garcia-Vidal F.J., Martin-Moreno L. *New J. Phys.*, **11**, 123020 (2009).
7. Nikitin A.Y., Garcia-Vidal F.J., Martin-Moreno L. *Phys. Status Solidi RRL*, **4**, 250 (2010).
8. Han Z., Bozhevolnyi S.I. *Rep. Prog. Phys.*, **76**, 016402 (2013).
9. Chang S.H., Gray S.K., Shatz G.C. *Opt. Express*, **13**, 3150 (2005).
10. De Abajo G.F.J., Sáenz J.J., Dolado J.S. *Opt. Lett.*, **14**, 7 (2006).
11. Ebbesen T.W., Degiron A. *Pure Appl. Opt.*, **7**, S90 (2005).
12. Kuznetsova T.I., Lebedev V.S. *Phys. Rev. E*, **78**, 016607 (2008).

13. Kuznetsova T.I., Lebedev V.S. *Phys. Rev. B*, **70**, 035107 (2004).
14. Kuznetsova T.I., Lebedev V.S. *JETP Lett*., **79**, 62 (2004) [*Pis'ma Zh. Eksp. Teor. Fiz*., **79**, 70 (2004)].
15. Kuznetsova T.I., Lebedev V.S. *Quantum Electron*., **32**, 727 (2002) [*Kvantovaya Electron*., **32**, 727 (2002)].
16. Kuznetsova T.I., Raspopov N.A. *Quantum Electron*., **42**, 87 (2012) [*Kvantovaya Electron*., **42**, 87 (2012)].
17. Raether H. *Surface Plasmons on Smooth and Rough Surfaces and on Gratings* (Berlin: Springer, 1988).
18. Romanov S.G., Korovin A.V., Regensburger A., Peschel U. *Adv. Mater*., **23**, 2515 (2011).
19. Romanov S.G., Vogel N., Bley K., Landfester K., Weiss C.K., Orlov S., Korovin A.V., Chuiko G.P., Regensburger A., Romanova A.S., Kriesch A., Peschel U. *Phys. Rev. B*, **86**, 195145 (2012).
20. Romanov S.G., Regensburger A., Korovin A.V., Romanova A.S., Peschel U. *Phys. Rev. B*, **88**, 125418 (2013).
21. Konopsky V.N., Alieva E.V. *Phys. Rev. Lett*., **97**, 253904 (2006).
22. Konopsky V.N., Alieva E.V. *Opt. Lett.*, **34**, 479 (2009).
23. Melentiev P.N., Afanasiev A.E., Kuzin A.A., Zablotskiy A.V., Baturin A.S., Balykin V.I. *Opt. Express*, **19**, 22743 (2011).
24. Treshin I.V., Klimov V.V., Melentiev P.N., Balykin V.I. *Phys. Rev. A*, **88**, 023832 (2013).
25. Kuznetsova T.I., Raspopov N.A. *JETP*, **118**, 395 (2014) [*Zh. Eksp. Teor. Fiz*., **145**, 455 (2014)].
26. Kuznetsova T.I., Raspopov N.A. *Quantum Electron*., **45**, 1055 (2015) [*Kvantovaya Electron*., **45**, 1055 (2015)].
27. Ziman J. *Principles of the Theory of Solids* (Cambridge: Cambridge University Press, 1972; Moscow: Mir, 1974).
28. Yariv A., Yeh P. *Optical Waves in Crystals* (New York: Wiley, 1984; Moscow: Mir, 1987).
29. Mantsyzov B.I. *Opt. Commun*., **189**, 275 (2001).
30. Landau L.D., Lifshits E.M. *Electrodynamics of Continuous Media* (New York: Pergamon Press, 1963; Moscow: Nauka, 1982).
31. http://refractiveindex.info.